JOURNAL OF SPACECRAFT AND ROCKETS
Vol. 31, No. 6, November–December 1994

Zonally Decoupled Direct Simulation Monte Carlo Solutions of Hypersonic Blunt-Body Wake Flows

Richard G. Wilmoth,* Robert A. Mitcheltree,† and James N. Moss‡
NASA Langley Research Center, Hampton, Virginia 23681-0001
and
Virendra K. Dogra§
ViGYAN, Inc., Hampton, Virginia 23666-0325

Direct simulation Monte Carlo (DSMC) solutions are presented for the hypersonic flow behind a blunt body in which the wake region is solved in a zonally decoupled manner. The forebody flow is solved separately using either a DSMC or a Navier-Stokes method, and the forebody exit-plane solution is specified as the inflow condition to the decoupled DSMC solution of the wake region. Results are presented for a 70-deg, blunted cone at flow conditions that can be accommodated in existing low-density wind tunnels with the Knudsen number (based on the base diameter) ranging from 0.03 to 0.001. The zonally decoupled solutions show good agreement with fully coupled DSMC solutions of the wake flow densities and velocities. The wake closure predicted by the zonally decoupled solutions is in better agreement with fully coupled results than that predicted by a fully coupled Navier-Stokes method, indicating the need to account for rarefaction in the wake for the cases considered. The combined use of Navier-Stokes for the forebody with a decoupled DSMC solution for the wake provides an efficient method for solving transitional blunt-body flows where the forebody flow is continuum and the wake is rarefied.

Nomenclature

Kn = Knudsen number
M = Mach number
R_b = base radius, m
R_c = corner radius, m
R_n = nose radius, m
Re = Reynolds number
S = distance along body, m
T = temperature, K
u = axial velocity, m/s
V_∞ = freestream velocity, m/s
x = axial distance from nose, m
y = radial distance from axis, m
γ = ratio of specific heats
λ = mean free path, m
ρ = density, kg/m^3

Subscripts

i = internal
ov = overall
slip = wall slip
t = translational
∞ = freestream condition

Introduction

THE prediction of near-wake flow structure behind blunt bodies is an important element in the design of aerobrakes because of the need to impose payload constraints based on wake closure.[1,2] Recent studies using the direct simulation Monte Carlo (DSMC) method have demonstrated the ability to make predictions at densities where the forebody flow could be mostly regarded as continuum flow.[2–4] In fact, at the higher densities of these studies, good agreement was shown with continuum predictions based on the Navier-Stokes equations. In these studies, the DSMC simulations were conducted such that the full forebody and wake zones were computed simultaneously, that is, in a fully coupled manner. However, because of the extremely large density variations between the forebody and wake zones, this approach places severe constraints on the simulation time steps and practical cell resolution that could be used in obtaining the wake solution. Also, large computational resources are required to obtain DSMC forebody solutions for such low Knudsen numbers. On the other hand, continuum solutions can be obtained much more efficiently, and, at sufficiently low Knudsen numbers, the Navier-Stokes solutions provide an accurate description of the flowfield in the forebody region. Therefore, a study was conducted to investigate the importance of coupling the forebody and wake zones and to investigate the adequacy of using a combined Navier-Stokes–DSMC method to solve the problem.

In rarefied and transitional flows, the need to maintain strong coupling between different flow regions is mainly caused by the lack of thermal equilibrium between the translational and internal modes. For blunt bodies, thermal nonequilibrium occurs mainly in the bow shock and in the wake region, where the local mean free path becomes large, as illustrated in Fig. 1. When the complete problem is solved using a fully coupled DSMC approach, these regions of nonequilibrium will be "captured" by the simulation. However, in order to decouple the forebody and wake solutions, an artificial boundary must be placed between the two regions, and flow properties from the forebody solution must be specified along this boundary in order to generate a solution for the wake. The difficulty is that, since the flow may not be in thermal equilibrium everywhere along this boundary, the velocity distribution may not be adequately defined by a Maxwell-Boltzmann distribution. In the DSMC method, the usual method of imposing a flow boundary condition is to introduce simulation particles sampled from an equilibrium distribution based on specified macroscopic mean-flow properties (temperature, density, and mean velocity).[5] Therefore, in regions of thermal nonequilibrium, the particles introduced will not have the proper distributions of velocity and internal energy. However, in practice, it may not be necessary to reproduce these distributions exactly in order to generate wake solutions of sufficient

Received July 28, 1993; revision received April 8, 1994; accepted for publication April 11, 1994.

*Aerospace Engineer, Aerothermodynamics Branch, Gas Dynamics Division. Senior Member AIAA.
†Aerospace Engineer, Aerothermodynamics Branch, Gas Dynamics Division. Member AIAA.
‡Aerospace Engineer, Aerothermodynamics Branch, Gas Dynamics Division. Fellow AIAA.
§Research Engineer. Senior Member AIAA.

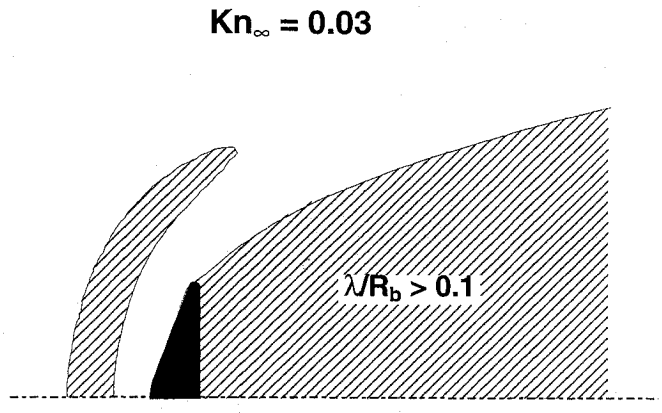

Fig. 1 Typical regions of rarefaction in low-density blunt-body flowfield.

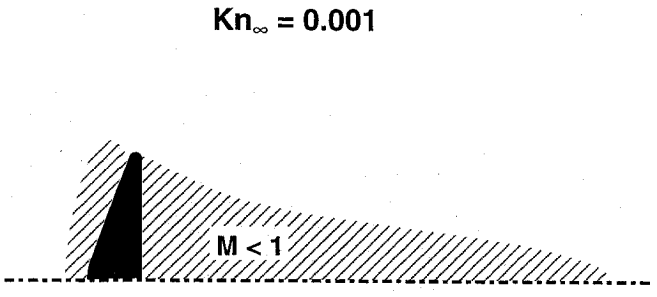

Fig. 2 Typical subsonic regions in hypersonic blunt-body flowfield.

accuracy for engineering studies if the mean-flow properties are preserved.

In the near-continuum regime, strong coupling is needed only in large regions of subsonic flow and possibly in regions where the local Knudsen number is relatively high. For blunt-body flows, subsonic regions occur behind the bow shock, in the wake, and in the boundary layer (Fig. 2). Thus, for continuum flows, a decoupled approach is justified if the boundary used to divide the forebody and wake zones is chosen so that the flow normal to the boundary is supersonic. It is usually adequate to ignore the subsonic portion of the boundary layer if it is thin in the direction along the decoupling boundary. It may be necessary to provide special treatment in the boundary layer to account for the significant velocity slip that can occur in the rapid expansion of the flow around the shoulder.

The purpose of the present study is to investigate the adequacy of a zonally decoupled approach for a range of hypersonic blunt-body flow conditions. In the context of this paper, "zonally decoupled" means that the forebody and wake regions are solved separately with no iterative feedback from the wake to the forebody. The motivation for using such an approach is to provide a more efficient method for performing parametric studies of different afterbody flows based on a single forebody solution. Results are presented for nitrogen flow about a 70-deg-half-angle, blunted cone with a base diameter of 5 cm (a wind-tunnel model of the Viking lander aeroshell[6]). Fully coupled DSMC solutions for this model are presented in Ref. 2. Fully coupled DSMC and Navier-Stokes forebody solutions from a similar study[4] are used to provide starting conditions for the zonally decoupled DSMC wake solutions. The zonally decoupled DSMC solutions are then compared with the fully coupled DSMC and the fully coupled Navier-Stokes solutions. The results presented focus on the overall wake flowfield structure, wake closure, and thermal nonequilibrium effects.

Computational Test Cases

Computational results are presented for a model size (Fig. 3) and flow conditions that can be accommodated in existing low-density hypersonic wind tunnels. The specific flow conditions are those that can be attained in the SR3 tunnel at Centre National de la Recherche Scientifique (CNRS)[7] and are listed in Table 1. Three cases were computed where the Knudsen number based on the model base diameter varied from about 0.03 to 0.001. Based on the results of Refs. 2 and 4, these conditions produce a large vortex in the wake at the two lower Knudsen numbers (cases 2 and 3), whereas no vortex is evident at the higher Knudsen number (case 1) when no sting or afterbody is present.

Table 1 Test conditions[a]

Case	ρ_∞, 10^{-5} kg/m^3	V_∞, m/s	T_∞, K	M_∞	Re^b_∞	Kn^b_∞
1	1.7	1502	13.3	20.2	768	0.032
2	5.2	1502	14.0	19.7	2,220	0.011
3	46.6	1633	15.0	20.6	20,600	0.001

[a]SR3 facility; nitrogen flow from conical nozzles; model temperature 300 K.
[b]Based on model diameter of 5 cm.

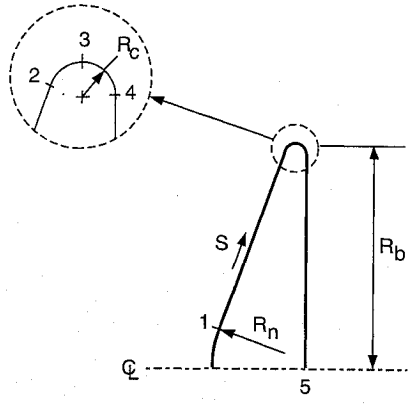

Fig. 3 Geometry of test model; $R_b = 0.025$ m.

Computational Approach

DSMC computations of the wake region were performed using initial mean-flow profiles from forebody solutions obtained using both DSMC and Navier-Stokes methods. The DSMC and Navier-Stokes methods and the approach used to generate the zonally decoupled solutions are described below.

DSMC Method

The DSMC method[5,8] models the discrete particle nature of the flow and is applicable across the range from continuum to free-molecular flows. However, the method is normally applied only in the transitional and free-molecular regimes, because the computing requirements can become prohibitive for continuum applications.

Molecular collisions were modeled using the variable hard sphere (VHS) molecular model while considering energy exchange between translational and rotational modes. All calculations were performed for a nonreacting gas with one chemical species (N_2). Because of the low total temperature, the simulations model the nitrogen flow as a nonreacting gas with energy exchange between rotational and translational modes. The surface temperature is assumed to be constant at 300 K, and the gas-surface interaction model is assumed to be diffuse with full thermal accommodation.

Continuum Method

The Langley aerothermodynamic upwind relaxation algorithm (LAURA) of Gnoffo[9,10] was used to generate the Navier-Stokes solutions. LAURA is an upwind-biased, point-implicit relaxation algorithm for obtaining the numerical solution to the governing equations for three-dimensional viscous hypersonic flows in thermochemical states ranging from perfect gas to both thermal and chemical nonequilibrium. For the results presented in this paper, only perfect-gas solutions about axisymmetric geometries were considered. A constant γ of 1.4 and a molecular weight of 28.0 were used to simulate the nonreacting flow of N_2.

For the zonally decoupled computations, LAURA is used to compute the forebody flow and DSMC is used to compute the wake flow. Fully coupled solutions of the complete forebody-wake regions are also given for comparison with the fully coupled and zonally decoupled DSMC solutions. Further details of the LAURA calculations are given in Ref. 4.

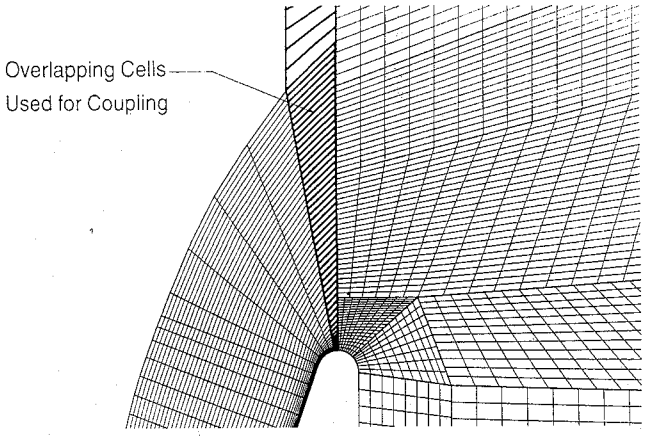

Fig. 4 Overlapping grid used in zonally decoupled solution.

For the LAURA forebody calculations used in the zonally decoupled DSMC simulations, no-slip surface boundary conditions are used. For the fully coupled LAURA calculations of the complete forebody-wake problem, slip boundary conditions are imposed using the method described in Ref. 11. This is necessary because of the high degree of velocity slip encountered at the shoulder of the body. However, since the zonally decoupled solutions are started upstream of this high-slip region, the no-slip LAURA solutions are considered to be adequate for providing the inflow conditions at the coupling boundary. Further discussion of the effects of slip is given later.

Zonally Decoupled Approach

For the zonally decoupled computations, DSMC and Navier-Stokes solutions of the forebody region were taken from the study of Ref. 4, and profiles were extracted for generating separate, decoupled DSMC wake solutions. These profiles were extracted at a vertical plane just upstream of the expansion corner of the base. The results from Ref. 4 indicate that the mean flow profiles along this plane are independent of the downstream conditions as indicated by comparison of the profiles for forebody-only and fully coupled forebody-wake solutions.

The decoupled wake solutions are generated using the same grid and computational parameters as those in the fully coupled solution. Therefore, any differences between the two DSMC solutions should only be the result of the decoupling. The last column of cells from the forebody grid is included, so that the wake grid effectively overlaps the forebody grid as shown in Fig. 4. The density, velocity, and temperature from the forebody solution are specified as the inflow condition at these overlapping cells. Simulation particles are introduced at each of these cells by sampling from a "streaming" Maxwellian distribution function. For the DSMC forebody solution, the translational and internal modes are not in equilibrium everywhere along this coupling boundary. Therefore, the specified temperature for the entering particle velocity and internal-energy distribution is based on an overall temperature that allows for both translational and internal degrees of freedom [$T_{ov} = (3T_t + f_i T_i)/(3 + f_i)$, where f_i is the number of internal degrees of freedom]. Use of a single temperature introduces errors in the velocity and energy distributions of entering particles when the translational and internal temperatures are different. To determine the sensitivity of the wake calculation to this approximation, simulation results are presented where separate translational and internal temperatures are used as inflow conditions. For the decoupled DSMC wake calculations that used the Navier-Stokes forebody results, the specification of a single temperature is consistent with the thermal-equilibrium gas model used in LAURA for these calculations. Although the LAURA code has a thermal-nonequilibrium model available, the model does not treat rotational nonequilibrium and was not considered to be appropriate for the low temperatures of the present study.

Results

In the results that follow, the fully coupled DSMC solution of the complete forebody-wake problem is used as the standard for comparison, since, in principle, it should be applicable across the entire range of test conditions computed. Comparisons with the fully coupled Navier-Stokes results are first discussed in order to demonstrate the need for DSMC in regions of the problem. Results are then presented that compare the zonally decoupled and fully coupled DSMC solutions of the wake flowfield. Some limited results assessing the effects of wall slip, thermal nonequilibrium, grid resolution, and location of the coupling boundary are then given.

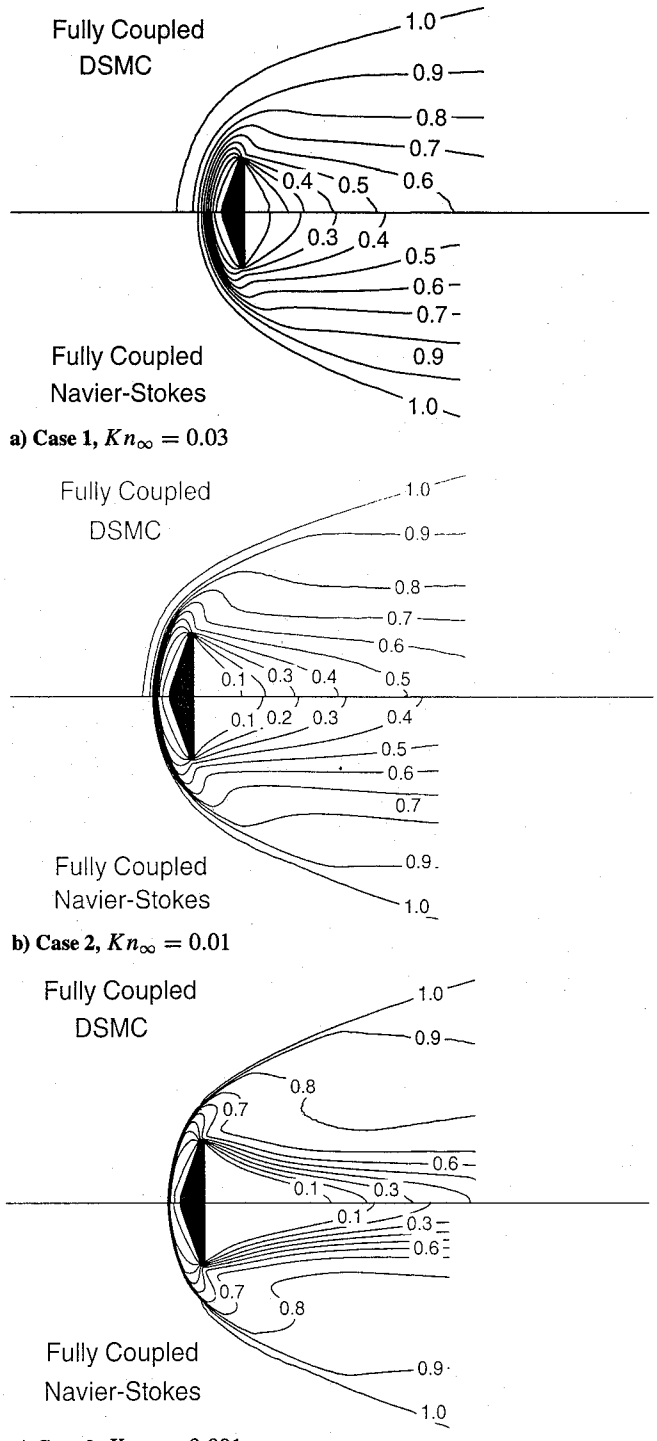

Fig. 5 Comparison of axial-velocity contours for fully coupled DSMC and Navier-Stokes (contour values nondimensionalized by freestream velocity).

Comparison of Fully Coupled DSMC and Navier-Stokes

Computational results are presented in Fig. 5 comparing contours of the axial velocity (nondimensionalized by the freestream

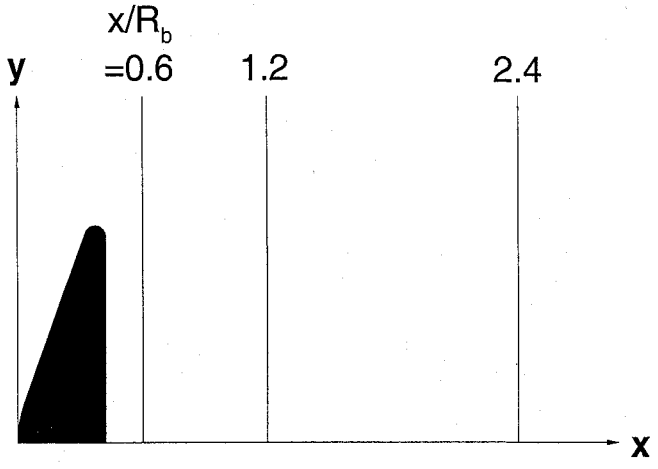

Fig. 6 Locations used to present wake profiles.

velocity). Axial-velocity contours are chosen because they exhibit clearly the closure of the wake. (Wake closure in this paper is defined to be the point at which the flow stagnates, i.e., has zero velocity along the axis.) The results show differences in both forebody and wake flowfields for the most rarefied condition (case 1), where the bow shock is thicker and the wake velocities are higher for the DSMC solution. However, for the most continuum-like condition (case 3), the DSMC and Navier-Stokes solutions agree quite well in the forebody region but still show differences in the wake. The results of Ref. 4 show that the two solutions give reasonable agreement for surface quantities (pressure and heat transfer) on the forebody for all three cases.

Density profiles at the three axial locations behind the body shown in Fig. 6 are given in Fig. 7. These profiles show a weaker, more diffuse bow shock predicted by DSMC for the more rarefied case (case 1), but show very good agreement between DSMC and Navier-Stokes predictions for the most continuum-like condition (case 3). However, there are differences in density directly behind the body for all three cases. The differences in predicted wake closure are shown by comparisons of the axial velocities along the centerline in Fig. 8. This figure shows that the DSMC calculations exhibit more rapid wake closure than the Navier-Stokes results for all three cases. These comparisons indicate the need to take account of rarefaction effects in the wake predictions for the present model and flow conditions. It should also be pointed out that the LAURA calculations exhibited marginal stability at the most rarefied condition (case 1). This is in contrast to the calculations of Ref. 4, which exhibited no such stability problems for case 1 when a sting was present. The nature of this stability problem is under investigation.

Comparison of Fully Coupled and Zonally Decoupled DSMC

Results are presented in Fig. 9 comparing axial-velocity contours for the fully coupled and zonally decoupled DSMC where the latter used the Navier-Stokes forebody solution. The forebody solutions are essentially the same as those shown in Fig. 5 except that the Navier-Stokes solutions are obtained without any coupling to the wake. The zonally decoupled DSMC solutions of the wake region show better agreement with the fully coupled DSMC results for all three cases than do the fully coupled Navier-Stokes results shown previously.

A more detailed comparison of the flowfields is given in Figs. 10 and 11, which show profiles of density and axial velocity. In these figures, the zonally decoupled results obtained using both the Navier-Stokes and the DSMC forebody solutions are shown. Again, the best agreement with the fully coupled DSMC is obtained for the lower Knudsen numbers. For the most rarefied case, there is some outward shift of the bow shock as a result of the decoupling. This shift is attributed to inaccuracies in preserving thermal-nonequilibrium effects across the coupling boundary with the decoupled approach. These effects are most evident in the density profiles for case 1, where use of the DSMC forebody results

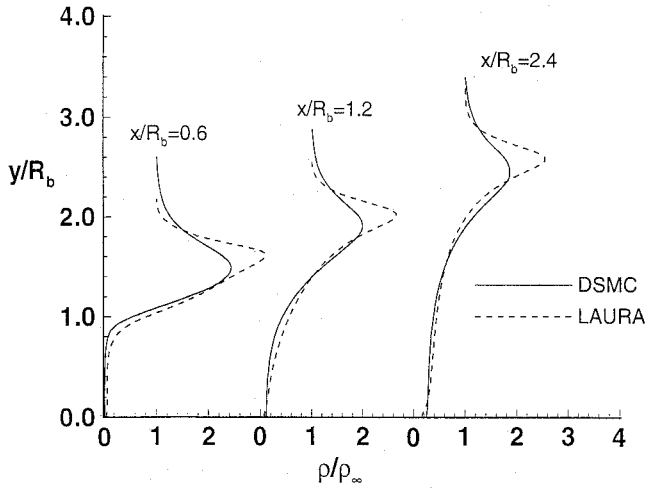

a) Case 1, $Kn_\infty = 0.03$

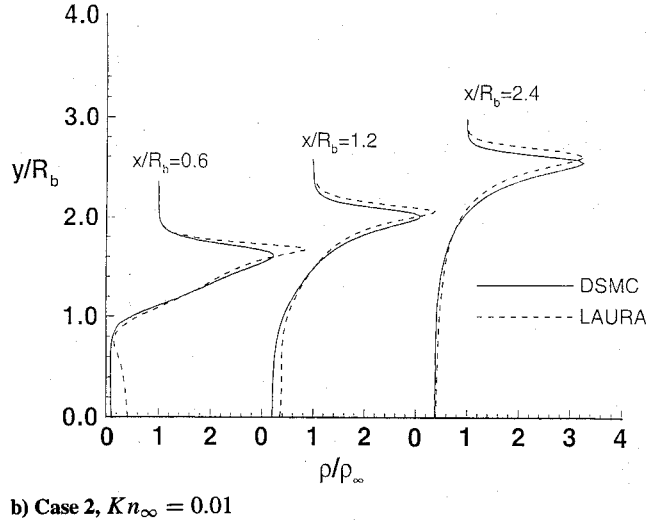

b) Case 2, $Kn_\infty = 0.01$

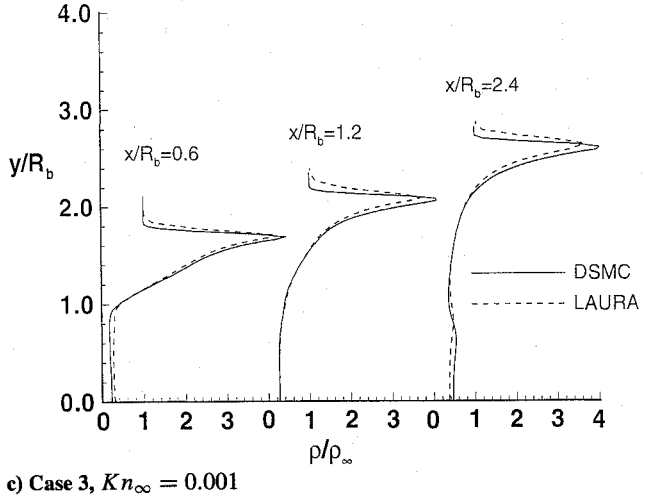

c) Case 3, $Kn_\infty = 0.001$

Fig. 7 Density profiles for fully coupled DSMC and Navier-Stokes solutions.

provides better agreement with the fully coupled results near the coupling boundary, while the use of the Navier-Stokes results seems to give better agreement farther downstream. These seemingly conflicting results simply point out the sensitivity of the bow shock to the initial conditions. Overall, the wake solutions are relatively insensitive to the forebody solution used. For all cases, there is very good agreement in the region immediately behind the body and excellent agreement in the velocity profiles.

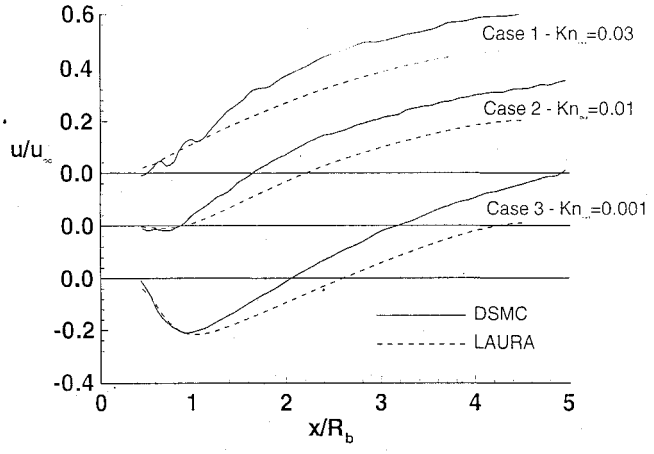

Fig. 8 Centerline axial-velocity distributions predicted by fully coupled DSMC and Navier-Stokes.

Figure 12 shows a comparison of the centerline velocities. The zonally decoupled solution gives very good agreement with the fully coupled results and is insensitive to whether DSMC or Navier-Stokes forebody solutions are used. Therefore, either method should be acceptable for engineering predictions where overall wake closure is of principal concern. Furthermore, the zonally decoupled method provides considerable computational savings for parametric studies (other afterbody geometries, grid refinements, etc.), since the forebody solution does not have to be repeated. When the Navier-Stokes forebody solution is used in the present test cases, the zonally decoupled solutions require less than one-half the total resources (memory and CPU time) required by comparable fully coupled DSMC calculations.

Slip Effects

The rapid expansion of the forebody flow around the shoulder of the body into the wake produces a sudden drop in density. This produces a local region where rarefaction effects are important even when the majority of the flowfield is continuum. These slip effects tend to reduce the extent of the wake, resulting in more rapid closure.[4]

A representation of this slip is given in Fig. 13, which shows the magnitude of the velocity tangent to the wall at the center of the first computational cell adjacent to the wall. Strictly speaking, this is not the "slip velocity," but since the cell size is generally of the order of a mean free path or less, it provides an estimate of the relative changes in slip along the body. All three test cases exhibit significant slip (on the order of 30 to 40% of the freestream velocity) on the shoulder of the body. While the degree of slip is small over most of the forebody, the trend toward an increase in slip as the Knudsen number increases is evident. A large degree of slip exists along the base even for the most continuum-like case, and the slip velocity is negative for cases 2 and 3 because of the recirculating flow.

A comparison of the slip velocities predicted by the zonally decoupled and fully coupled approaches is shown in Fig. 14. Since the zonally decoupled solutions are started upstream of the point of maximum slip, the rapid increase in slip is still predicted, the maximum slip being about the same as with the fully coupled method. This is particularly important for the zonally decoupled solutions that used the no-slip Navier-Stokes forebody results and indicates that neglecting the small amount of wall slip ahead of the shoulder should not significantly affect the wake results.

Thermal-Nonequilibrium Effects

The degree of thermal nonequilibrium varies considerably for the three cases and is illustrated in Fig. 15 by profiles of $(T_t - T_i)/T_{ov}$, where T_t is the translational temperature, T_i is the internal temperature, and T_{ov} is the overall temperature. Since the zonally decoupled solutions are started assuming an equilibrium distribution of velocities and internal energies at the same overall temperature, the degree of nonequilibrium is artificially set to zero at the inflow boundary. However, in the region of the bow shock, the departure from equilibrium is caused by the steep gradients across the shock, and the nonequilibrium behavior is quickly reestablished as the flow develops downstream of the coupling boundary. For the more continuum-like cases, the zonally decoupled solutions agree with the fully coupled results, since the difference between translational and internal temperatures is much less.

To further assess the sensitivity of the zonally decoupled solutions to the modeling of the thermal nonequilibrium, a separate calculation was performed for the most rarefied case (case 1), in which both the translational and internal temperatures were specified from the DSMC solution over the forebody. A comparison of

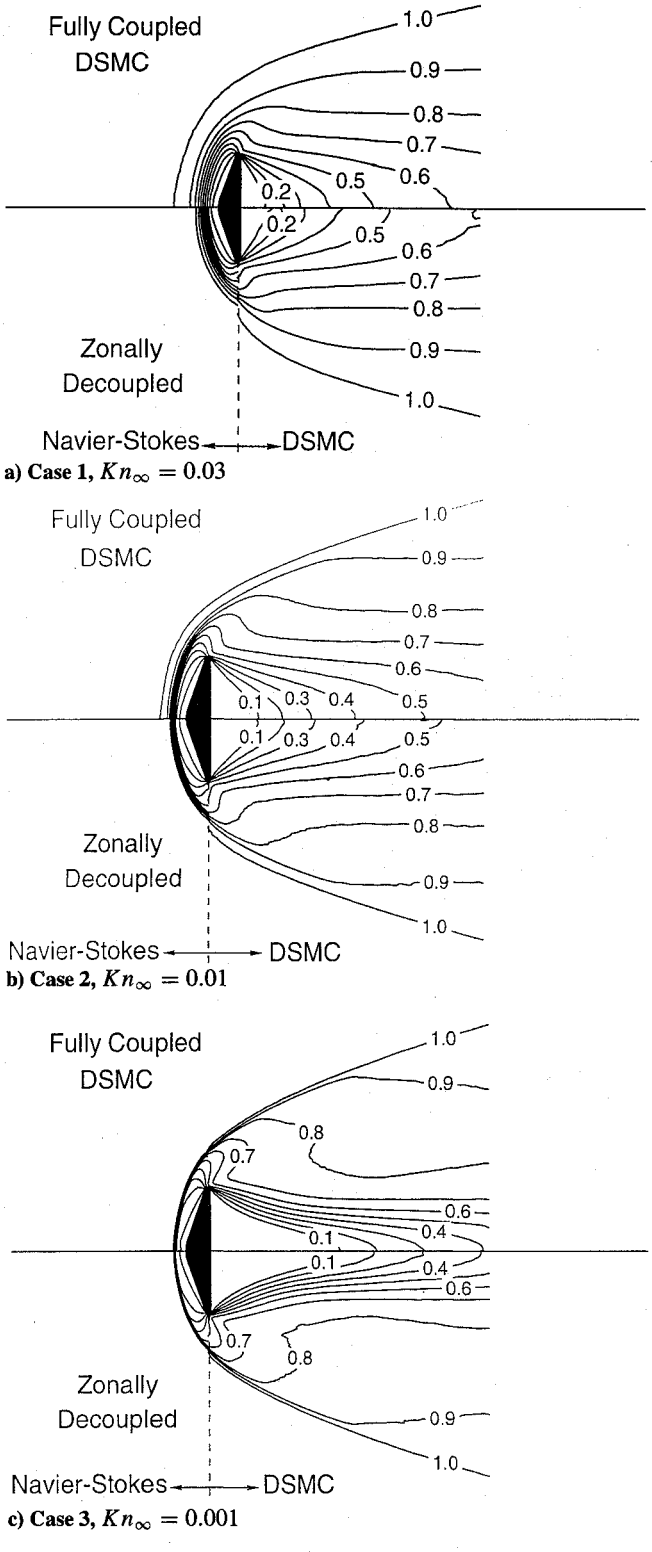

Fig. 9 Comparison of fully coupled and zonally decoupled DSMC predictions of axial-velocity contours.

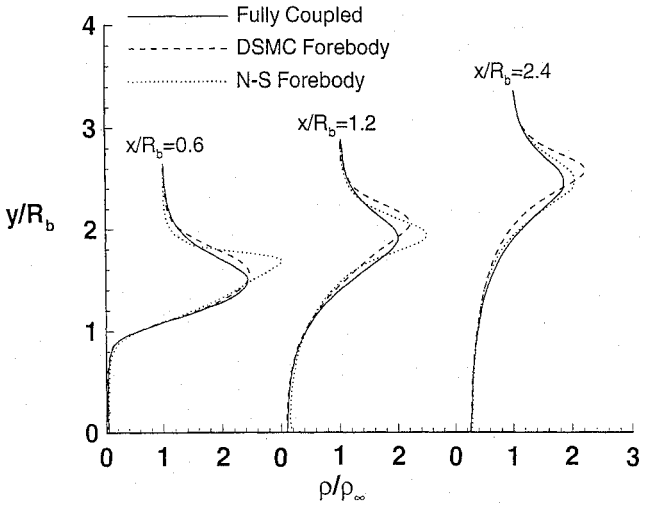

a) Case 1, $Kn_\infty = 0.03$

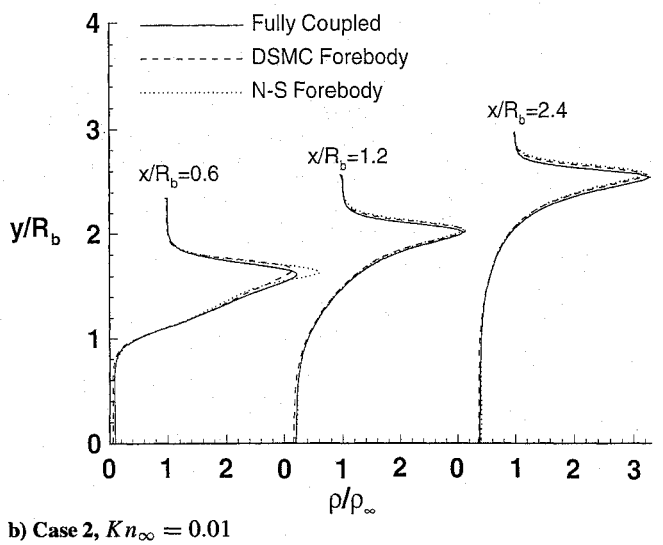

b) Case 2, $Kn_\infty = 0.01$

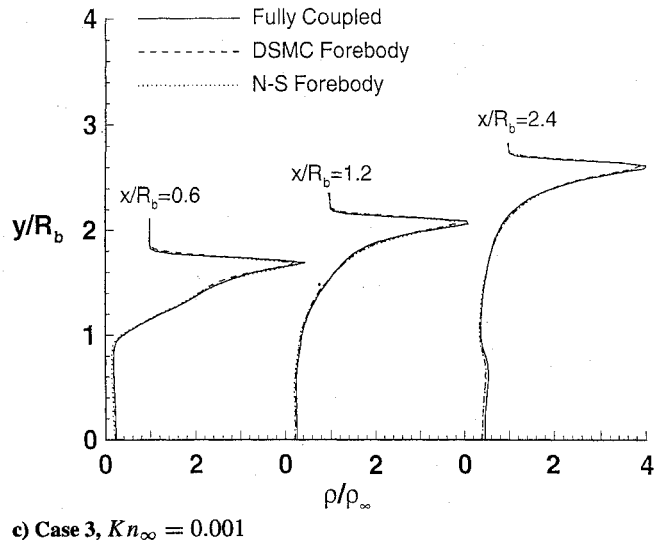

c) Case 3, $Kn_\infty = 0.001$

Fig. 10 Density profiles predicted by fully coupled and zonally decoupled DSMC.

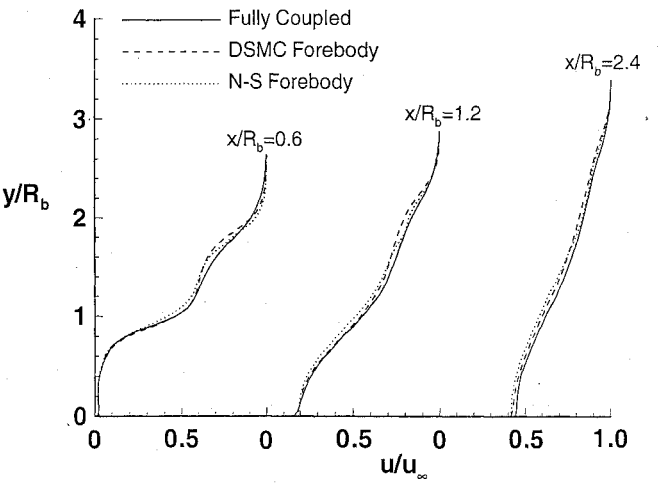

a) Case 1, $Kn_\infty = 0.03$

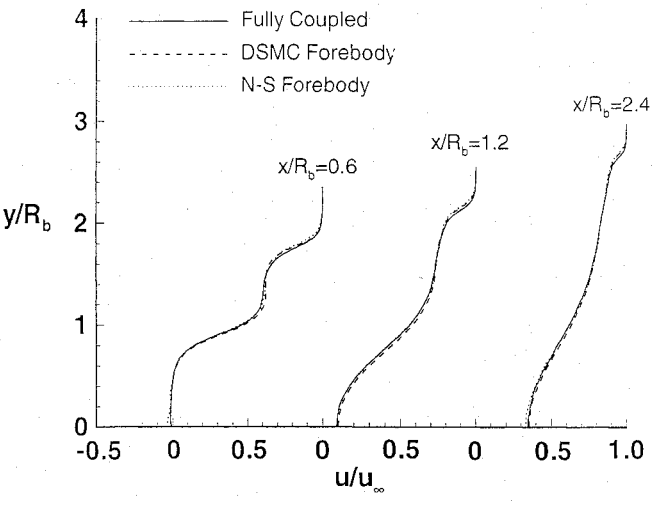

b) Case 2, $Kn_\infty = 0.01$

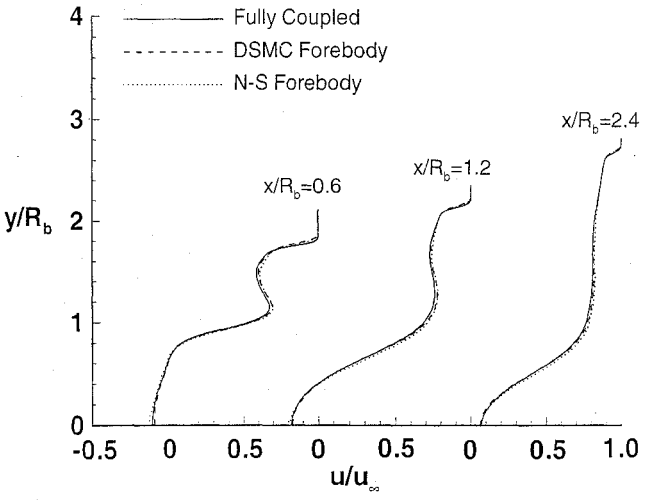

c) Case 3, $Kn_\infty = 0.001$

Fig. 11 Axial-velocity profiles predicted by fully coupled and zonally decoupled DSMC.

profiles of density, velocity, and nonequilibrium temperature ratios is shown in Fig. 16. The density and velocity profiles show little effect of specifying both temperatures. However, the degree of thermal nonequilibrium agrees much better in the bow shock, but shows poorer agreement immediately behind the body, especially for the profile closest to the inflow boundary.

Grid Refinement

One advantage of using the zonally decoupled approach is that it requires less computational resources to compute just the wake region. Therefore, it is more feasible to perform parametric studies such as grid refinement. For the present test cases, the adequacy of the grid size for DSMC simulations is questionable for the most continuum-like test case (case 3). To perform a grid refinement

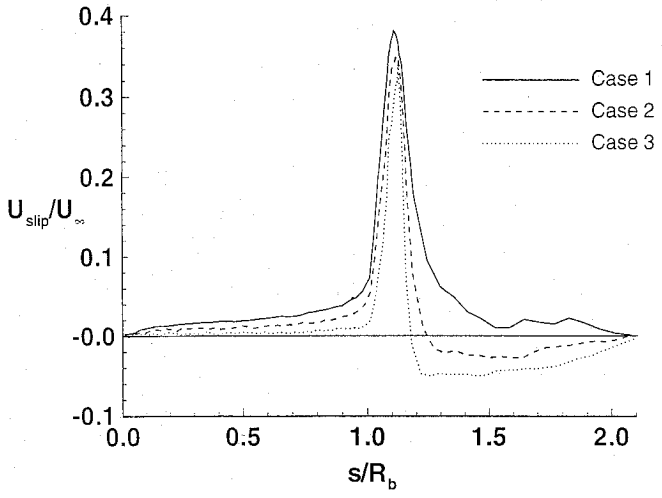

Fig. 12 Comparison of centerline velocities predicted by fully coupled and zonally decoupled DSMC.

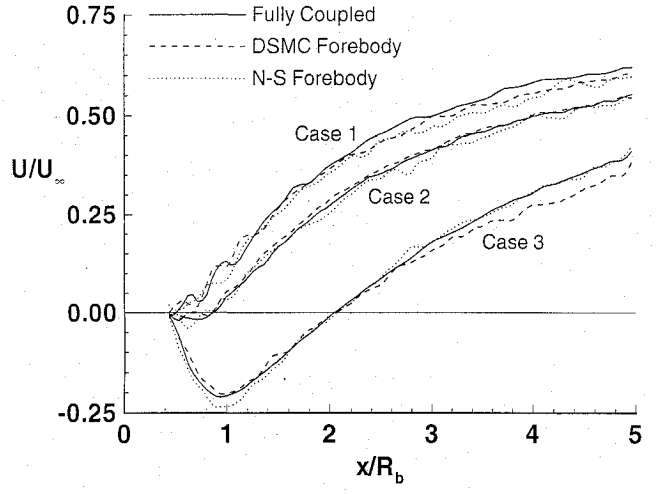

Fig. 13 Wall slip velocity predicted by fully coupled DSMC.

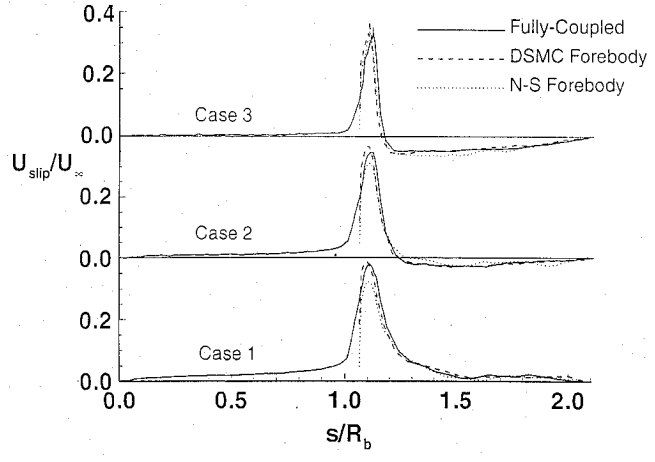

Fig. 14 Comparison of wall slip predicted by fully coupled and zonally decoupled DSMC.

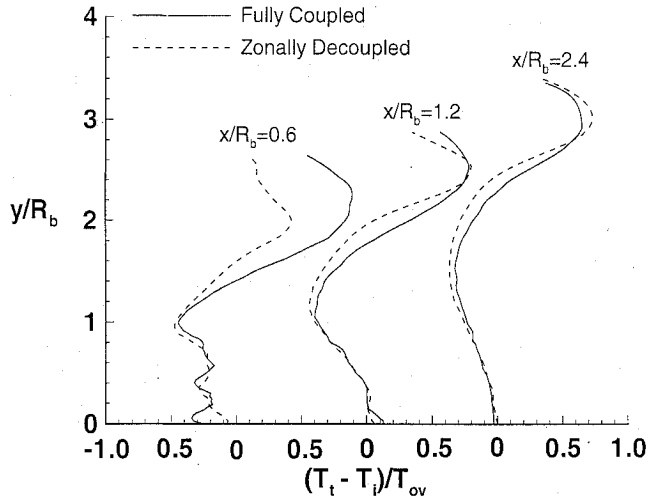

a) Case 1, $Kn_\infty = 0.03$

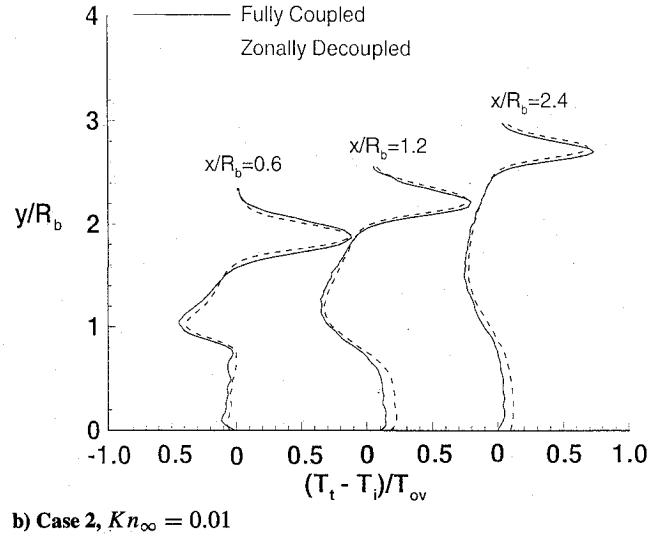

b) Case 2, $Kn_\infty = 0.01$

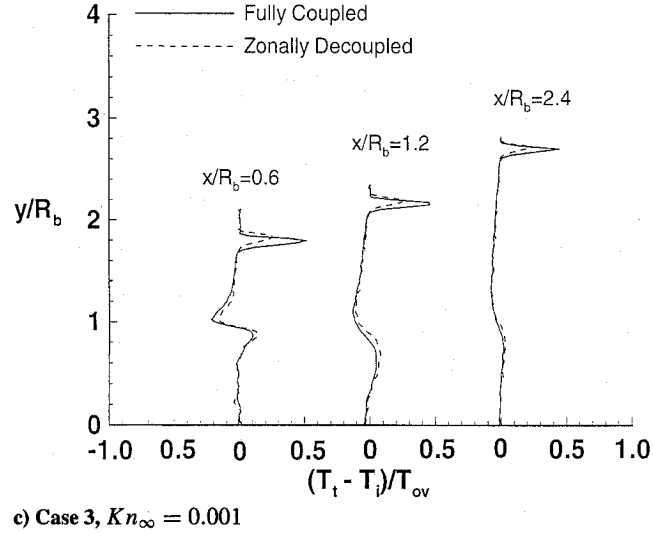

c) Case 3, $Kn_\infty = 0.001$

Fig. 15 Profiles showing degree of thermal nonequilibrium predicted by fully coupled and zonally decoupled methods.

study for the complete wake region would have required very large computational resources. Therefore, separate simulations were performed for case 3 in which only a region immediately behind the body was simulated. These simulations used mean-flow profiles obtained from the zonally decoupled solution of the complete wake region that were specified as input in the same manner as described previously where a single overall temperature was used. Two simulations were performed: one using the same grid as the full wake simulation, and the second using a grid with twice as many cells in each coordinate direction (four times as many total cells in the wake). The refined grid was imposed immediately behind the body and extended to $x/R_b \approx 2.8$ to enclose the recirculation region.

The overall similarities in the vortex structure between the fully coupled results and those from the reduced simulation with the refined grid are shown in the streamline plot given in Fig. 17. A comparison of the centerline velocities in the wake for the refined grid with those for the fully coupled simulation is given in Fig. 18. It is seen that the reduced simulation gives the same overall wake

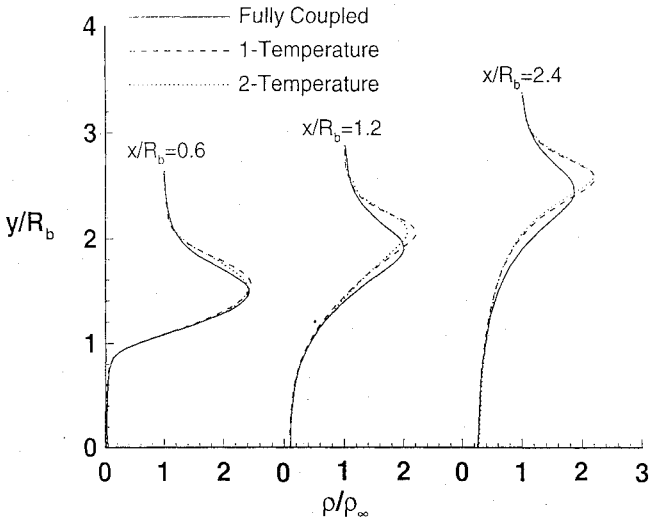

a) Density

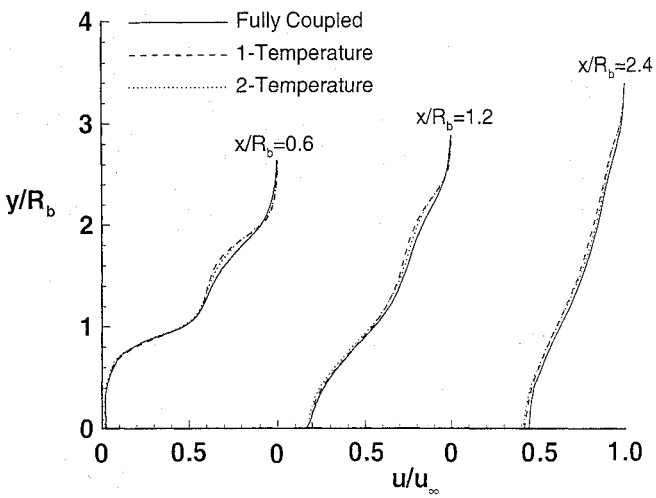

b) Axial velocity

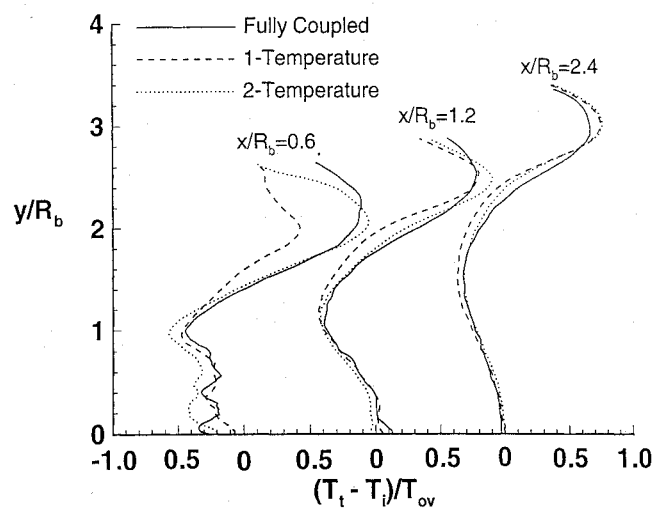

c) Nonequilibrium temperature ratio

Fig. 16 Comparison of profiles predicted with one-temperature and two-temperature methods (case 1, $Kn_\infty = 0.03$).

structure as the fully coupled simulation, and that the extent of the recirculating region is not changed by refining the grid. Based on these results, it should be possible to perform even more detailed simulations of the wake region (e.g., to resolve details of the vortex structure and more detailed afterbody geometries) without requiring unreasonable amounts of computational resources.

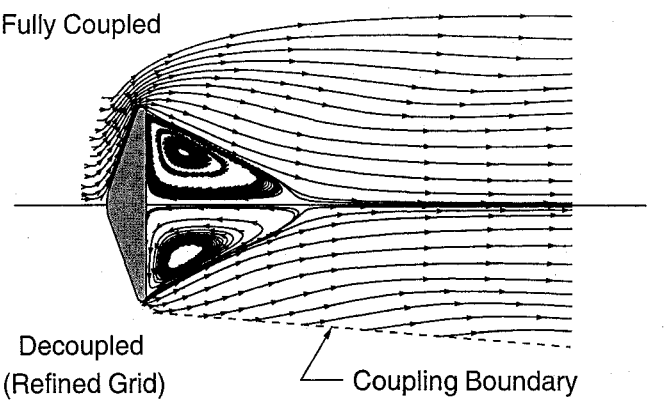

Fig. 17 Comparison of wake streamlines for fully coupled solution and zonally decoupled solution obtained with refined grid (case 3, $Kn_\infty = 0.001$).

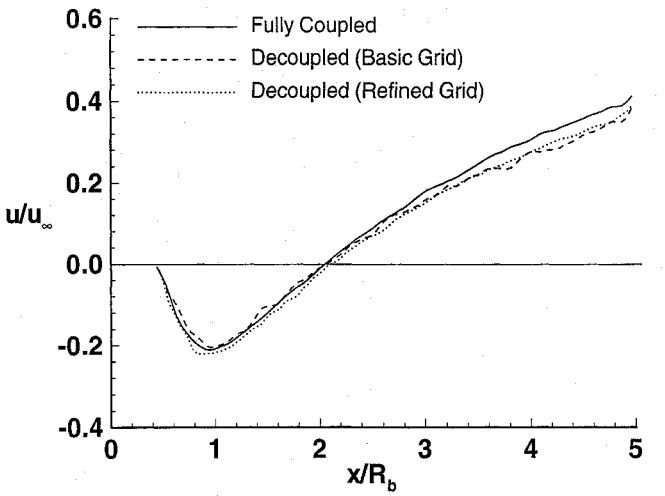

Fig. 18 Effect of grid refinement on wake closure predicted with zonally decoupled DSMC (case 3, $Kn_\infty = 0.001$).

Concluding Remarks

Zonally decoupled DSMC solutions of the wake region behind blunt bodies in hypersonic flow have been shown to be a viable approach for predicting the overall mean-flow properties in the wake over a range of wind-tunnel test conditions. For the conditions examined, the use of either a DSMC or Navier-Stokes solution of the forebody provided an adequate inflow condition for predicting the wake closure with a separate, decoupled DSMC simulation. At freestream conditions where the forebody flow exhibits significant rarefaction effects, it is preferable to use the DSMC solution for the forebody to account for thermal-nonequilibrium effects. However, for the conditions examined, these nonequilibrium effects did not have a significant effect on the mean-flow wake properties. Of course, for problems where thermal behavior is of primary importance, such as in the prediction of radiation, the nonequilibrium nature should be simulated as accurately as possible, and the errors introduced by zonal decoupling might be unacceptable.

The principal advantage of the zonally decoupled approach is computational efficiency. For the cases presented, the computational resources for the zonally decoupled solutions are less than one-half those for the fully coupled solutions when the Navier-Stokes forebody solutions are used. Furthermore, the zonally decoupled approach is found to be useful in performing parametric studies such as grid refinement, where even greater computational resources would be needed to solve the complete problem. By isolating the region of interest, it is possible to perform such studies in a fraction of the time required to solve the full problem.

In the present study, no attempt was made to optimize the shape or location of the artificial boundary along which the forebody and wake solutions were decoupled. Further work to define the opti-

mum conditions for selecting such a boundary and to define a more accurate method for simulating nonequilibrium effects across this boundary would be useful. Such work could be especially useful in developing a fully hybrid approach in which the Navier-Stokes and DSMC methods are combined in a more strongly coupled manner and where the DSMC simulation is restricted to that portion of the flowfield where significant rarefaction effects occur.

References

[1]Gnoffo, P. A., Price, J. M., and Braun, R. D., "Computation of Near-Wake, Aerobrake Flowfields," *Journal of Spacecraft and Rockets*, Vol. 29, No. 2, 1992, pp. 182–189.

[2]Dogra, V. K., Moss, J. N., and Price, J. M., "Near Wake Structure for a Generic ASTV Configuration," AIAA Paper 93-0271, Jan. 1993.

[3]Lumpkin, F. E., III, Boyd, I. D., and Venkatapathy, E., "Comparison of Continuum and Particle Simulations of Expanding Rarefied Flows," AIAA Paper 93-0728, Jan. 1993.

[4]Moss, J. N., Mitcheltree, R. A., and Dogra, V. K., "Hypersonic Blunt Body Wake Computations Using DSMC and Navier-Stokes Solutions," AIAA Paper 93-2807, July 1993.

[5]Bird, G. A., *Molecular Gas Dynamics*, Clarendon Press, Oxford, 1976.

[6]Blanchard, R. C., and Walberg, G. D., "Determination of the Hypersonic Continuum/Rarefied Flow Drag Coefficient of the Viking Lander Capsule Aeroshell from Flight Data," NASA TP-1793, Dec. 1980.

[7]Allegre, J., "The SR3 Low Density Wind-Tunnel: Facility Capabilities and Research Development," AIAA Paper 92-3972, July 1992.

[8]Bird, G. A., "Monte-Carlo Simulation in an Engineering Context," edited by Sam S. Fisher, Vol. 74, Part 1, *Progress in Astronautics and Aeronautics: Rarefied Gas Dynamics*, 1981, pp. 239–255.

[9]Gnoffo, P. A., Gupta, R. N., and Shinn, J. L., "Conservation Equations and Physical Models for Hypersonic Air Flows in Thermal and Chemical Nonequilibrium," NASA TP-2867, Feb. 1989.

[10]Gnoffo, P. A., "An Upwind-Biased, Point-Implicit Relaxation Algorithm for Viscous, Compressible Perfect-Gas Flows," NASA TP-2953, Feb. 1990.

[11]Gupta, R. N., Scott, C. D., and Moss, J. N., "Slip Boundary Equations for Multicomponent Nonequilibrium Airflow," NASA TP-2452, Nov. 1985.